Official Journal of the Asian Pacific Society of Respirology
Respirology

ORIGINAL ARTICLE

Fibroblast–matrix interplay: Nintedanib and pirfenidone modulate the effect of IPF fibroblast-conditioned matrix on normal fibroblast phenotype

GALI EPSTEIN SHOCHET,[1] LUTZ WOLLIN[2] AND DAVID SHITRIT[1,3]

[1]*Pulmonary Medicine Department, Meir Medical Center, Kfar Saba, Israel;* [2]*Immunology & Respiratory Diseases Research, Boehringer Ingelheim, Biberach, Germany;* [3]*Sackler Faculty of Medicine, Tel Aviv University, Tel Aviv, Israel*

ABSTRACT

Background and objective: **Idiopathic pulmonary fibrosis (IPF) is a progressive lung disease with poor prognosis. Activated fibroblasts are the key effector cells in fibrosis, producing excessive amounts of collagen and extracellular matrix (ECM) proteins. Whether the ECM conditioned by IPF fibroblasts determines the phenotype of naïve fibroblasts is difficult to explore.**

Methods: **IPF-derived primary fibroblasts were cultured on Matrigel and then cleared using ammonium hydroxide, creating an IPF-conditioned matrix (CM). Normal fibroblast CM served as control. Normal fibroblasts were cultured on both types of CM, and cell count, cell distribution and markers of myofibroblast differentiation; transforming growth factor beta (TGFβ) signalling; and ECM expression were assessed. The effects of the anti-fibrotic drugs nintedanib and pirfenidone at physiologically relevant concentrations were also explored.**

Results: **Normal fibroblasts cultured on IPF-CM arranged in large aggregates as a result of increased proliferation and migration. Moreover, increased levels of pSmad3, pSTAT3 (phospho signal transducer and activator of transcription 3), alpha smooth muscle actin (αSMA) and Collagen1a were found, suggesting a differentiation towards a myofibroblast-like phenotype. SB505124 (10 µmol/L) partially reversed these alterations, suggesting a TGFβ contribution. Furthermore, nintedanib at 100 nmol/L and, to a lesser extent, pirfenidone at 100 µmol/L prevented the IPF-CM-induced fibroblast phenotype alterations, suggesting an attenuation of the ECM–fibroblast interplay.**

Conclusion: **IPF fibroblasts alter the ECM, thus creating a CM that further propagates an IPF-like phenotype in normal fibroblasts. This assay demonstrated differences in drug activities for approved IPF drugs at clinically relevant concentrations. Thus, the matrix–fibroblast phenotype interplay might be a relevant assay to explore drug candidates for IPF treatment.**

Correspondence: Gali Epstein Shochet, Pulmonary Medicine Department, Meir Medical Center, 59 Tchernichovsky Street, Kfar Saba 44281, Israel. Email: gali.epstein@clalit.org.il

Received 12 November 2017; invited to revise 18 December 2017; revised 20 December 2017; accepted 01 February 2018 (Associate Editor: Darryl Knight; Senior Editor: Chris Grainge).

Key words: extracellular matrix, fibroblasts, idiopathic pulmonary fibrosis, in vitro techniques, transforming growth factor beta.

SUMMARY AT A GLANCE

We developed an assay using Idiopathic pulmonary fibrosis (IPF) and normal primary fibroblasts. The IPF-fibroblast-conditioned matrix (CM) induced fibroblast to myofibroblast transition (FMT) with transforming growth factor beta (TGFβ) and signal transducer and activator of transcription 3 (STAT3) pathway activation in normal cells. This assay demonstrated differences in drug activities for newly approved IPF drugs (nintedanib and pirfenidone) at clinically relevant concentrations.

Abbreviations: αSMA, alpha smooth muscle actin; ACTA2, Alpha-actin-2; CM, conditioned matrix; COL1A, Collagen1a; DDW, double-distilled water; ECM, extracellular matrix; FN1, fibronectin 1; GAPDH, glyceraldehyde 3-phosphate dehydrogenase; IPF, idiopathic pulmonary fibrosis; MMP, matrix metalloproteinase; PFD, pirfenidone; pSTAT3, phospho STAT3; STAT3, signal transducer and activator of transcription 3; TGFβ, transforming growth factor beta; TGFβR, TGFβ receptor.

INTRODUCTION

Idiopathic pulmonary fibrosis (IPF) is a chronic and fatal disease characterized by a progressive decline in lung function.[1] The pulmonary interstitial fibroblast is the main cell responsible for the alteration of the collagen metabolism and other extracellular matrix (ECM) proteins, which characterize pulmonary fibrosis.[2] Fibroblasts and myofibroblasts accumulate in IPF lungs in 'fibroblastic foci' as they are the predominant sites of excessive matrix production. They are assumed to be the leading edge of active fibrosis.[3] The ECM is a dynamic structure that contributes to organ integrity and function, and its regulation of cell phenotype is a major aspect of cell biology.[4] The ECM proteins (e.g. collagen, laminin and fibronectin) and all their fragmented forms all have biological functions.[4,5] It is

well established that the microenvironment plays a significant role in disease progression.[6] In the lung, ECM plays an active role in shaping cell behaviour both in health and disease.[7]

Nintedanib is approved for the treatment of IPF.[8] It has shown consistent anti-fibrotic and anti-inflammatory activity in animal models of lung fibrosis[9] and interference with central processes in fibrosis, such as fibroblast proliferation, migration and differentiation, and the secretion of ECM proteins.[10] The second approved anti-fibrotic agent is pirfenidone, which was shown to prevent fibrosis progression in a variety of animal models (reviewed in Ref.[11]) as well as in clinical trials.[12] However, the effect of these anti-fibrotic agents on the interplay between the microenvironment and the phenotypic development of fibroblasts was not assessed.

Based on previously described methods,[13,14] we developed an in vitro test system using primary fibroblasts from IPF patients and control donors to generate a conditioned matrix (CM), which enables the exploration of ECM changes on fibroblast phenotype and signalling. We tested the involvement of the transforming growth factor beta (TGFβ) signalling cascade and the effect of nintedanib and pirfenidone on the interplay between the CM and fibroblast phenotype.

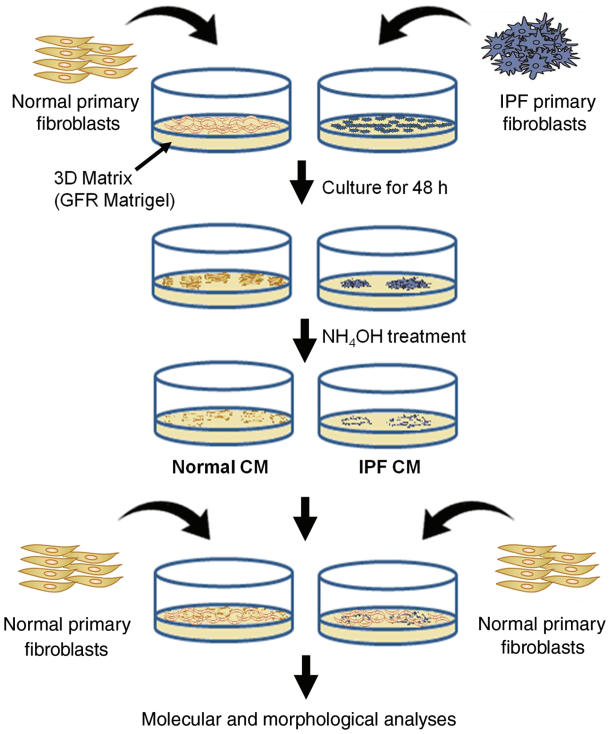

Figure 1 The CM model system. CM, conditioned matrix; GFR, growth factor reduced; IPF, idiopathic pulmonary fibrosis.

METHODS

Primary fibroblast culture

Primary human lung fibroblasts were isolated from at least six IPF (histologically confirmed) tissues and six control samples (histologically normal lung distant from the resected tumour), as described by Epstein Shochet *et al.*[15] The tissue was obtained at the time of biopsy. Following their extraction, the fibroblasts were cultured in Dulbecco's Modified Eagle's Medium (DMEM) supplemented with 20% FCS, L-glutamine (2 mmol/L) and antibiotics (Biological Industries, Kibbutz Beit-Haemek, Israel) and maintained in 5% CO_2 at 37°C. Fibroblasts of both IPF patients and control donors had typical spindle morphology and were vimentin- and alpha smooth muscle actin (αSMA)-positive and keratin-negative. The study was approved by the institutional Ethics Committee of Meir Medical Center (study number 0016-16-MMC). Signed informed consent was obtained from all patients.

Inhibitors

Inhibitors used were TGFβ receptor (TGFβR) inhibitor SB505124 (10 μmol/L, Sigma-Aldrich, St. Louis, MO, USA), nintedanib (100 nmol/L, Boehringer Ingelheim, Germany) and pirfenidone (100 μmol/L, Sigma Aldrich). Inhibitors were dissolved in dimethyl sulphoxide (DMSO). The same concentration of DMSO served as control.

CM preparation

IPF or control fibroblasts were cultured in 24-well plates previously coated with 10 mg/mL growth factor-reduced (GFR) Matrigel (BD Biosciences, Befrord, MA, USA) (Fig. 1). After 48 h, cells were removed by washing with: (i) double-distilled water (DDW) for 15 min; (ii) ammonium hydroxide, NH_4OH (0.06%, diluted in DDW; Sigma Aldrich) for 10 min; (iii) DDW briefly; and (iv) culture media. Then, normal fibroblasts (15×10^4) were added for further culture.

Visual assessment of the fibroblast distribution

Cultures were examined using the Olympus IX71 microscope (Olympus, Tokyo, Japan). Aggregate size and number, as well as the single cell number, were measured by ImageJ (National Institutes of Health, Bethesda, MD, USA; http://rsbweb.nih.gov/ij/).

The absolute fibroblast cell number/well was counted by the MACSQuant Analyzer (Miltenyi Biotec, Bergisch Gladbach, Germany) and the Nucleoview NC-200 (ChemoMetec, Allerod, Denmark).

RNA extraction, RT cDNA synthesis and real-time quantitative PCR

RNA was extracted using the RNeasy kit (Qiagen, Hilden, Germany). Extracted RNA was converted to cDNA using GeneAmp (Applied Biosystems, Inc., Foster City, CA, USA). PCR were obtained using Power SYBR Green (Thermo Fisher Scientific, Vilnius, Lithuania). Primer sequences (purchased from Hylabs, Rehovot, Israel) are listed in Table 1. GAPDH served as housekeeping control.

Western blotting and gelatin zymography

Western blot was performed as previously described.[14] The following antibodies were used: total Smad3 (Cell Signaling Technology, Danvers, MA, USA), phospho-Smad3 (pS423/425), Collagen1a, αSMA and GAPDH

Table 1 List of primers

	Forward (5′-3′)	Reverse (5′-3′)
FN1	CCTGCAAGCCCATAGCTGA	CCACGTTTCTCCGACCACAT
MMP2	CAAGGACCGGTTTATTTGGC	ATTCCCTGCGAAGAACACAGC
MMP9	CCTGGGCAGATTCCAAACCT	CAAAGGCGTCGTCAATCACC
GAPDH	CTCTGCTCCTCCTGTTCGAC	TTAAAAGCAGCCCTGGTGAC
ACTA2	TGAGAAGAGTTACGAGTTGCCTGAT	GCAGACTCCATCCCGATGAA
COL1A	CGAAGACATCCCACCAATCAC	CAGATCACGTCATCGCACAAC
TGFB1	TTTTGATGTCACCGGAGTTG	AACCCGTTGATGTCCACTTG

ACTA2, Alpha-actin-2; COL1A, Collagen1a; FN1, fibronectin 1; MMP, matrix metalloproteinase; TGF, transforming growth factor.

(Abcam, Cambridge, MA, USA). The results were normalized to GAPDH.

Gelatin zymography was performed as previously described.[14] Cell culture supernatants (24 μL) were electrophoresed at non-reducing conditions. Coomassie blue staining allowed visualization of clear lysis zones against the blue background. The results were normalized to background values.

Statistical analysis

Paired Student's t-tests were employed to analyse differences between the cohorts. An effect was considered significant when the *P*-value was ≤0.05. All experiments were conducted at least three times.

RESULTS

IPF-CM induces fibroblast cell migration and tubule-like structure organization

IPF fibroblasts were cultured on Matrigel for 48 h and then removed using NH_4OH, leaving the 'IPF-CM'. Normal tissue-derived fibroblasts were cultured in parallel wells for the 'normal CM' preparation, which served as control (see *Methods* section and Fig. 1). Then, normal fibroblasts were added to both CM. Soon after the addition of the fibroblasts to the IPF-CM (1–2 h), they started to migrate. After 2–3 h, tubule-like formations could be observed (Fig. 2A), and 24 h later, the cells organized in very large aggregates (800% increase, Fig. 2A,B; $P < 0.05$). A modest increase in cell number was observed after 24 h (Fig. 2C; $P < 0.05$). However, it could not account for the significant elevation in aggregate size. In addition, there was a significant reduction in the number of single cells (Fig. 2D; $P < 0.05$). These parameters were all previously described as markers of cell migration.[14]

Matrix metalloproteinases (MMP) are known to be important facilitators of cell invasion. MMP2 and MMP9 levels in the culture media measured after 24 h were elevated, supporting the increased cell migration/invasion rates (Fig. 2E,F). Moreover, the MMP2 mRNA levels in these cells cultured were significantly elevated (163% elevation, $n = 4$, $P < 0.01$, MMP9 level was not changed).

IPF-CM increases the fibrogenic potential of normal fibroblasts

Fibrotic tissue-derived fibroblasts are known to express higher levels of αSMA and Collagen1a (COL1A). Fibrosis is characterized by excessive accumulation of ECM components that primarily include collagen type I.[16] To test whether the IPF-CM modified normal cell behaviour towards a more 'IPF-like' phenotype, we tested the expression of these proteins in cells following their culture on the IPF-CM aSMA (ACTA2). Indeed, both were found to be significantly elevated in comparison to the control (Fig. 3A,B). Moreover, the ACTA2 and COL1A mRNA levels were elevated, along with fibronectin 1 (FN1) ($P < 0.05$; Fig. 3C). These changes were accompanied by morphological changes of the normal cells that presented with a more mesenchymal characteristic after 2 h (i.e. elongated shape; Fig. 2A upper right panel).

TGFβ pathway mediates IPF-CM-induced phenotype changes

The TGFβ pathway was extensively studied and found to be a key pathway in IPF.[17] TGFβ1 pathway involvement in mediating the phenotypic changes of fibroblasts cultured on IPF-CM was confirmed as the cells displayed increased levels of pSmad3 (Fig. 4A; $P < 0.05$) and TGFβ1 mRNA (20% elevation, $n = 4$, SD = 0.08, $P < 0.05$).

As a next step, a TGFβR inhibitor (SB505124) was added to the normal fibroblasts 1 h before their addition to the CM, and the effect of the IPF-CM was re-evaluated. A significant, but not complete, reduction in aggregate size was observed (Fig. 4B,C; $P < 0.05$). In addition, the elevation in total cell count and the reduction in the number of single cells were completely prevented (Fig. 4D,E; $P < 0.05$). The TGFβ pathway was also found to be involved in MMP2 and MMP9 activity levels as they were both significantly reduced following exposure to the TGFβR inhibitor (1.05 relative expression following SB505124 addition, $P < 0.05$). Furthermore, the MMP2 mRNA expression levels in the cells cultured on the IPF-CM were also reduced (Fig. 4F; $P < 0.05$), further supporting TGFβ pathway activation as MMP2 is a known target of pSmad3.

IPF-CM partially increases the fibrogenic potential of normal fibroblasts via the TGFβ pathway

Once canonical TGFβ pathway activation was established, we explored whether it also controls the elevated expression levels of αSMA and Collagen1a. The expression of these fibrogenic markers was tested after

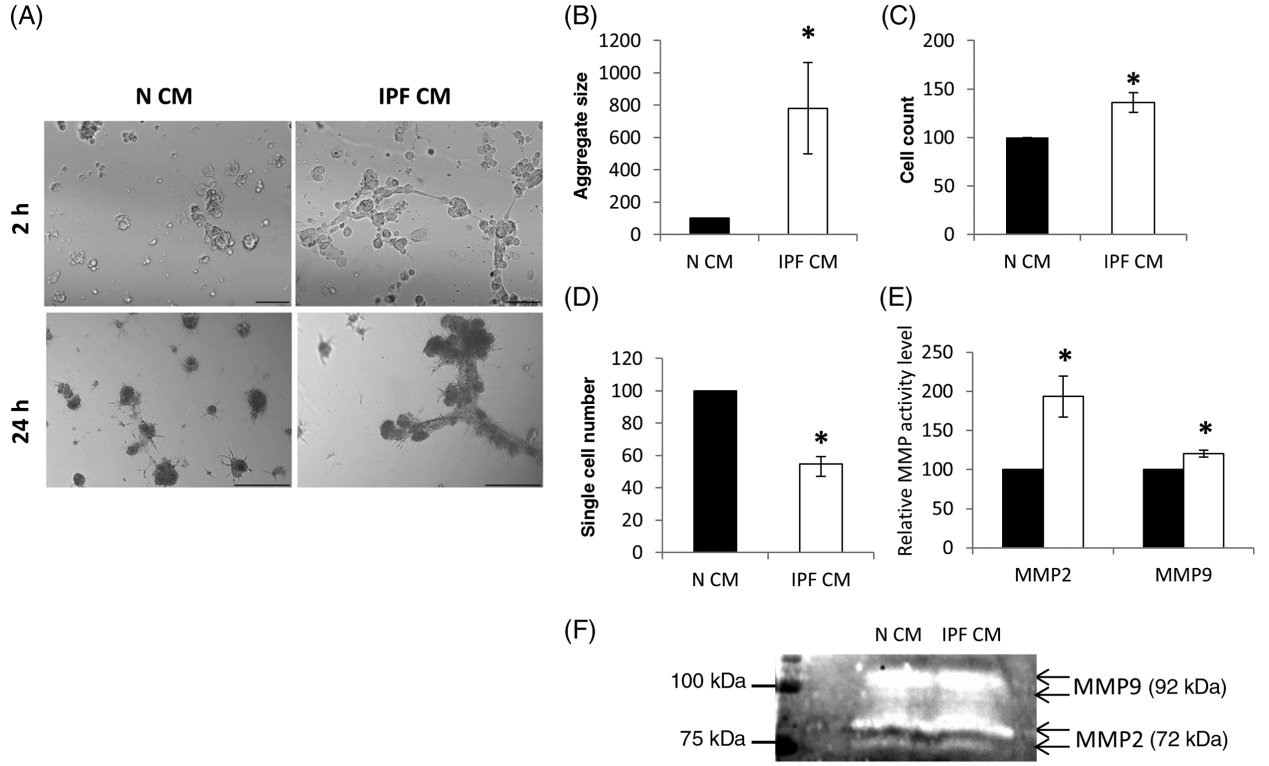

Figure 2 Idiopathic pulmonary fibrosis-conditioned matrix (IPF-CM) affects normal fibroblast phenotype. Normal fibroblasts were cultured on control (N)/IPF-CM for 3 and 24 h. (A) Representative photomicrographs of normal fibroblasts cultured on N/IPF-CM for 3 h (×10 magnification, bar represents 50 μm) and 24 h (×4 magnification, bar represents 500 μmol/L). (B–D) Following culture, cells were counted, and cell distribution was evaluated (n = 8). (E,F) Matrix metalloproteinase (MMP) activity in the culture media was tested by gelatin zymography (n = 7); arrows indicate the active (lower) and the proenzyme (upper) forms for each MMP. Results were normalized to control and considered significant (*) if $P < 0.05$. ■, N-CM; □, IPF-CM.

24 h of culture on the N/IPF-CM with/without SB505124. Collagen1a was significantly inhibited at the protein and mRNA levels (Fig. 4F,G; $P < 0.05$). In addition, ACTA2 and FN1 were reduced at the mRNA level (Fig. 4F; $P < 0.05$). Nevertheless, the αSMA protein expression was not affected by TGFβR blockage (Fig. 4F). These results suggest that the canonical TGFβ-pSmad3 signalling is prominently, but not solely,

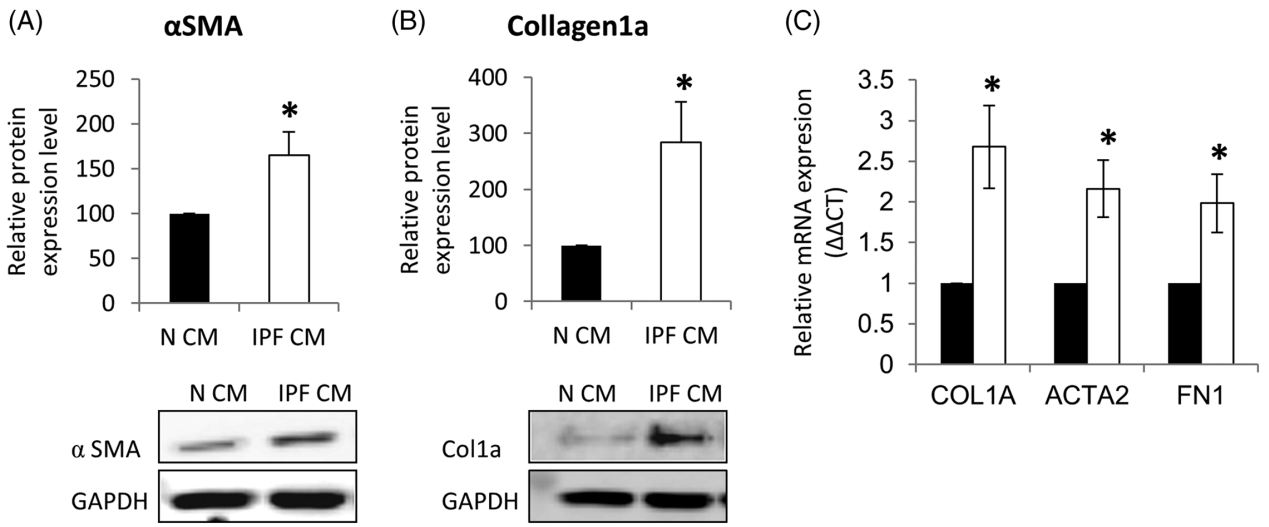

Figure 3 Idiopathic pulmonary fibrosis-conditioned matrix (IPF-CM) increases the fibrogenic potential of normal fibroblasts. Normal fibroblasts were cultured on control (N)/IPF-CM. Following 24 h culture, cells were harvested for protein/RNA extraction, and the effect of IPF-CM on alpha smooth muscle actin (αSMA) (A) and Collagen1a (B) levels was tested by western blotting (n = 14). (C) The mRNA levels of Collagen1a (COL1A), ACTA2 and fibronectin 1 (FN1) were evaluated by quantitative PCR (n = 5). Results were normalized to control and considered significant (*) if $P < 0.05$. ■, N-CM; □, IPF-CM.

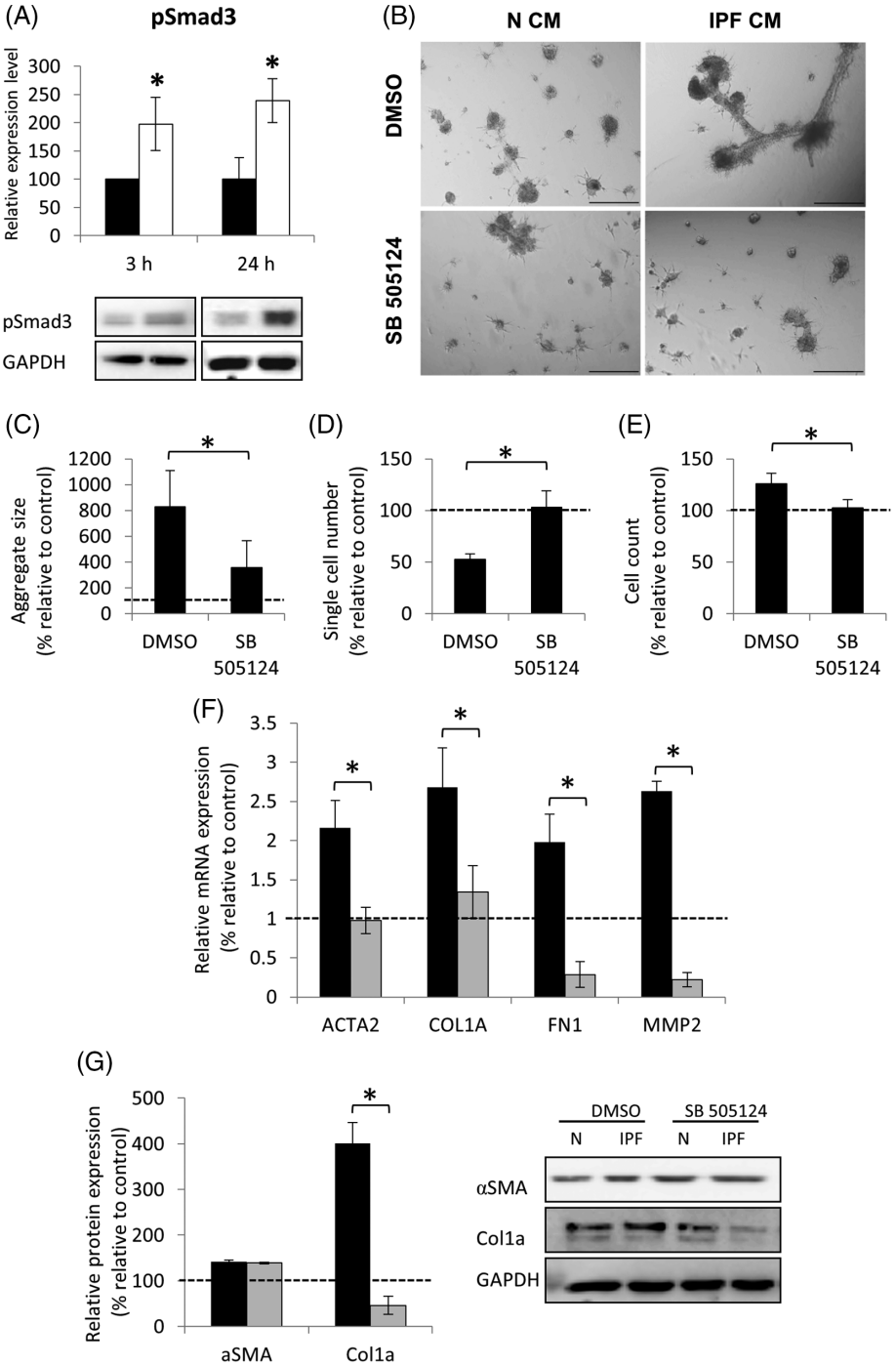

Figure 4 Transforming growth factor beta (TGFβ) pathway mediates the phenotype changes induced by the idiopathic pulmonary fibrosis-conditioned matrix (IPF-CM). Normal fibroblasts were cultured on control (N)/IPF-CM with/without SB 505124 (10 μmol/L) for 3 and 24 h. (A) Following culture, cells were harvested for RNA/protein extraction, and the effect of IPF-CM on pSmad3 levels was tested by western blotting (n = 5). ■, N-CM; □, IPF-CM. (B) Representative photomicrographs of normal fibroblasts cultured on N/IPF-CM with/without SB 505124 for 24 h (×4 magnification, bar represents 500 μm). (C–E) Following culture, aSMA (ACTA2) cell distribution was visually evaluated, and cells were counted (n = 8). (F) The effect of TGFβ pathway inhibition on IPF-CM induction of Collagen1a (COL1A), ACTA2, fibronectin 1 (FN1) and matrix metalloproteinase (MMP) 2 was evaluated by quantitative PCR (n = 4). (G) Alpha smooth muscle actin (αSMA) and COL1A protein levels were tested by western blotting (n = 5). ■, dimethyl sulphoxide (DMSO); □, SB 505124. Results were normalized to control and considered significant (*) if $P < 0.05$.

involved in the phenotypic changes of fibroblasts observed in this system.

IPF-CM leads to indirect pSmad3 activation

Smad3 can be activated indirectly by various pathways.[16] In order to verify successful inhibition, we tested pSmad3 levels following SB505124 addition at 3 and 24 h. We found that, as expected, the inhibitor completely reduced pSmad3 levels at 3 h (78% relative expression following SB505124 treatment, n = 4, SD = 32, $P < 0.05$). However, at 24 h, the inhibition was not complete (150% relative expression following SB505124 treatment, n = 5, SD = 50, $P = 0.07$), suggesting another signalling pathway involvement, possibly signal transducer and activator of transcription 3 (STAT3). Indeed, elevated levels of pSTAT3-Tyr705 were found in cells cultured on the IPF-CM after 3 h (123% elevation, n = 3, SD = 48, $P < 0.05$).

The anti-fibrotic drugs nintedanib and pirfenidone modulate the effect of IPF-CM on fibroblasts

To test whether the currently approved drugs to treat IPF, nintedanib and pirfenidone, can prevent the

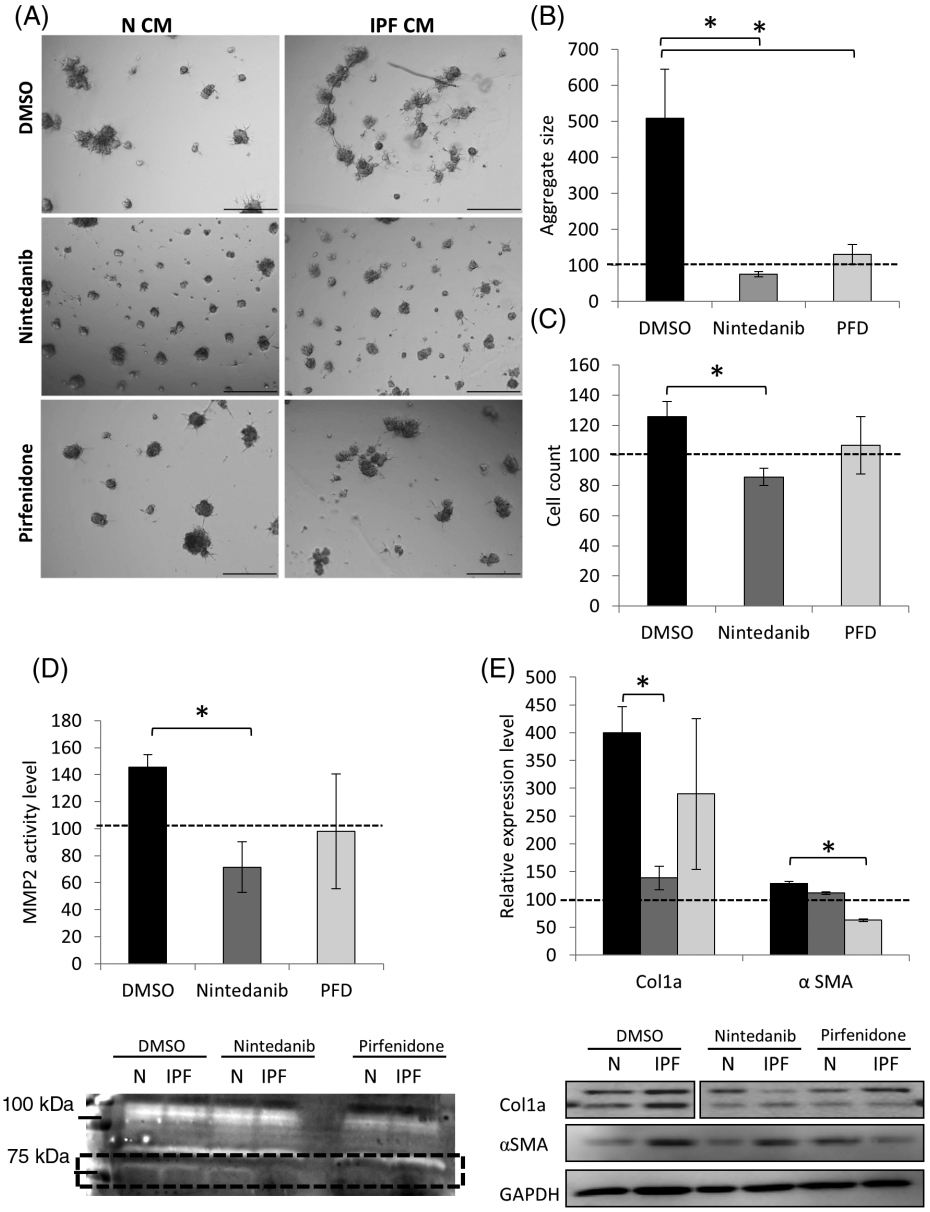

Figure 5 The anti-fibrotic drugs nintedanib and pirfenidone (PFD) modulate the effect of idiopathic pulmonary fibrosis-conditioned matrix (IPF-CM) on fibroblasts. Normal fibroblasts were cultured on control (N)/IPF-CM with/without nintedanib (100 nmol/L) or PFD (100 μmol/L) for 24 h. (A) Representative photomicrographs of normal fibroblasts cultured on N/IPF-CM with/without nintedanib or PFD for 24 h (×4 magnification, bar represents 500 μm). (B,C) Following culture, cell distribution was visually evaluated and cells were counted (n = 6). (D) Following culture, media was collected and matrix metalloproteinase (MMP) activity was tested by gelatin zymography (n = 4); broken line frame shows the activated MMP2 form. (E) Following culture, cells were harvested for protein extraction, and the effect of IPF-CM on alpha smooth muscle actin (αSMA) and Collagen1a (Col1a) levels was tested by western blotting (n = 6). Results were normalized to control and considered significant (*) if $P < 0.05$. ■, dimethyl sulphoxide (DMSO); ■, nintedanib; □, PFD.

effects of the IPF-CM on normal fibroblasts, we exposed the fibroblasts to nintedanib (100 nmol/L) or pirfenidone (100 μmol/L) for 1 h prior to their addition to the IPF-CM.

Both drugs effectively blocked the large aggregate formation (Fig. 5A,B; $P< 0.05$). Nintedanib completely blocked the elevation in total cell count and increased MMP2 activity (Fig. 5C,D; $P < 0.05$), as well as the elevation in MMP2 mRNA (1.16 relative expression following nintedanib addition, $P < 0.05$). Pirfenidone had fewer significant effects, although similar trends were observed (Fig. 5C,D). In addition, the exposure of fibroblasts to nintedanib completely prevented the increase in Collagen1a (Fig. 5E; $P < 0.05$), while pirfenidone (100 μmol/L) was effective in significantly reducing the αSMA levels (Fig. 5E; $P< 0.05$).

DISCUSSION

The ECM is a highly dynamic complex that composes the non-cellular aspect of tissues. In addition to providing structural integrity, ECM delivers important signals to drive cellular phenotypes. Within the lung interstitium, resident fibroblasts are the most commonly identified cells responsible for ECM production; they also serve as effector cells during injury repair.[7]

Unlike fibroblasts cultivated in planar (2D) dishes, cells within the normal 3D microenvironment extend membrane protrusions in all dimensions. Studies demonstrated distinct cell phenotypes between the 2D and 3D environments,[18] as well as differences in how cells might respond to therapeutic compounds.[19] Therefore, the importance of 3D models is clear, and the need for

reproducible in vitro biological systems is widely accepted.[19]

In this study, we created an IPF-CM. This system enables the study of IPF cell-induced ECM changes on normal fibroblasts. Previous studies demonstrated that IPF fibroblasts display a more fibrotic phenotype, which appears to remain following in vitro culture.[20] In fact, the IPF-CM induced normal fibroblast migration and elevated MMP2 activity that resulted in significant fibroblast aggregation on the IPF-CM. Moreover, αSMA and Collagen1a expression levels were increased. A recent study by Parker *et al.,*[21] which used decellularized ECM prepared from IPF lungs, highlighted the notion that diseased IPF ECM propagates fibrosis by a positive feedback loop between the diseased ECM and fibroblasts. This concept aligns well with the characteristic pattern of contiguous spreading during IPF progression.

In both tissue repair and tumorigenesis, TGFβ represents the prototypic inducer of myofibroblast differentiation. Therefore, interfering with TGFβ signalling currently poses one of the main therapeutic approaches for fibrosis and cancer.[22] We found that TGFβ pathway blockage reduced aggregation, Collagen1a protein expression and ACTA2 and FN1 mRNA levels, as well as MMP2 activity and mRNA expression. These results confirm previous studies reporting the strong link between TGFβ signalling and myofibroblast differentiation.[16,23] Although ACTA2 levels were significantly reduced by the TGFβR inhibitor, αSMA protein levels were not affected. As previously demonstrated, TGFβ treatment of lung fibroblasts, expressing high levels of αSMA, did not affect αSMA expression significantly,[24] indicating the involvement of other signalling pathways.

As myofibroblasts produce large amounts of ECM proteins, such as type I collagen, fibronectin and MMP, they contribute to the scarring of the tissue[25] and to its increased stiffness. Recent data support the hypothesis that ECM stiffness in IPF promotes a profibrotic phenotype in fibroblasts, such as myofibroblast differentiation,[3] matrix synthesis[21,26] and downregulation of anti-fibrotic molecules.[26] Indeed, recent reports suggested that ECM protein translation in IPF is positively influenced by the IPF ECM, even in fibroblasts derived from normal donors.[21] Although important, this aspect was not investigated in the current work.

Smad3 was shown to be the major contributor in regulating myofibroblast differentiation.[17] While the early (3 h) pSmad3 activation was completely blocked by SB505124, it was not blocked at 24 h. O'Reilly *et al.* suggested[16] that pSmad3 could be indirectly activated by STAT3, which was also shown to induce several morphological features consistent with a myofibroblast phenotype.[27,28] Furthermore, Pechkovsky *et al.* reported that IPF fibroblasts express high levels of pSTAT3-Y705 in comparison to control fibroblasts.[29] Indeed, significant pSTAT3 activation was observed in the cells cultured on the IPF-CM by an unknown trigger.

In the last part of this work, we evaluated the effect of currently available anti-fibrotic drugs nintedanib and pirfenidone on the CM–fibroblast interplay to qualify our assay system for drug testing. These experiments were performed at concentrations that are within the range of the clinical exposure achieved in IPF patients after steady-state standard dosing.[11,30,31] While both drugs significantly reduced the large aggregate formation, nintedanib was more effective than pirfenidone in inhibiting increased cell counts, Collagen1a expression and MMP2 activity. However, nintedanib at 100 nmol/L did not significantly reduce αSMA. This is in agreement with previous studies demonstrating αSMA inhibition by nintedanib at much higher concentrations (2 μmol/L).[32] Contrary to nintedanib, pirfenidone significantly reduced αSMA at 100 μmol/L. To the best of our knowledge, we are the first to demonstrate such in vitro effects for this drug at this dose.

Compared to several in vitro studies conducted with nintedanib[32–34] and pirfenidone[35–38] at excessively high concentrations, in our newly developed assay, we demonstrated drug activities and differences between the two drugs in the range of the clinical exposure concentrations. Hence, the demonstrated CM–fibroblast phenotype interplay might be a relevant assay format to explore further drug candidates for IPF treatment. In this study, we did not aim to identify the trigger driving the demonstrated IPF-CM effects on the fibroblast phenotype. However, extracellular proteins attached to the IPF-CM or the potentially altered CM stiffness might be exciting directions for future studies.

In conclusion, IPF fibroblasts modify the ECM differently than normal fibroblasts, thus creating a CM that further propagates the 'IPF-like' phenotype of normal fibroblasts. We suggest a model of IPF progression in which an initial insult creates a small fibrotic region in the lung ECM, which corrupts nearby fibroblasts, which further remodel the surrounding lung tissue, spreading the fibrosis.

Acknowledgement

The authors thank Tatiana Epstein for English editing.

Disclosure statement

L.W. is an employee of Boehringer Ingelheim, the inventor of the drug nintedanib used in this study. The study was funded, in part, by Boehringer Ingelheim, Biberach, Germany.

REFERENCES

1 Raghu G, Collard HR, Egan JJ, Martinez FJ, Behr J, Brown KK, Colby TV, Cordier JF, Flaherty KR, Lasky JA *et al.*; ATS/ERS/JRS/ALAT Committee on Idiopathic Pulmonary Fibrosis. An official ATS/ERS/JRS/ALAT statement: idiopathic pulmonary fibrosis: evidence-based guidelines for diagnosis and management. *Am. J. Respir. Crit. Care Med.* 2011; **183:** 788–824.

2 Booth AJ, Hadley R, Cornett AM, Dreffs AA, Matthes SA, Tsui JL, Weiss K, Horowitz JC, Fiore VF, Barker TH *et al.* Acellular normal and fibrotic human lung matrices as a culture system for in vitro investigation. *Am. J. Respir. Crit. Care Med.* 2012; **186**: 866–76.

3 Scotton CJ, Chambers RC. Molecular targets in pulmonary fibrosis: the myofibroblast in focus. *Chest* 2007; **132**: 1311–21.

4 Oskarsson T. Extracellular matrix components in breast cancer progression and metastasis. *Breast* 2013; **22**(Suppl. 2): S66–72.

5 Marom B, Rahat MA, Lahat N, Weiss-Cerem L, Kinarty A, Bitterman H. Native and fragmented fibronectin oppositely

modulate monocyte secretion of MMP-9. *J. Leukoc. Biol.* 2007; **81**: 1466–76.
6 Pietras K, Ostman A. Hallmarks of cancer: interactions with the tumor stroma. *Exp. Cell Res.* 2010; **316**: 1324–31.
7 White ES. Lung extracellular matrix and fibroblast function. *Ann. Am. Thorac. Soc.* 2015; **12**(Suppl. 1): S30–3.
8 Richeldi L, du Bois RM, Raghu G, Azuma A, Brown KK, Costabel U, Cottin V, Flaherty KR, Hansell DM, Inoue Y *et al.*; INPULSIS Trial Investigators. safety of nintedanib in idiopathic pulmonary fibrosis. *N. Engl. J. Med.* 2014; **370:** 2071–82.
9 Wollin L, Maillet I, Quesniaux V, Holweg A, Ryffel B. anti-inflammatory activity of the tyrosine kinase inhibitor nintedanib in experimental models of lung fibrosis. *J. Pharmacol. Exp. Ther.* 2014; **349**: 209–20.
10 Wollin L, Wex E, Pautsch A, Schnapp G, Hostettler KE, Stowasser S, Kolb M. Mode of action of nintedanib in the treatment of idiopathic pulmonary fibrosis. *Eur. Respir. J.* 2015; **45**: 1434–45.
11 Schaefer CJ, Ruhrmund DW, Pan L, Seiwert SD, Kossen K. Antifibrotic activities of pirfenidone in animal models. *Eur. Respir. Rev.* 2011; **20**: 85–97.
12 Azuma A. Pirfenidone treatment of idiopathic pulmonary fibrosis. *Ther. Adv. Respir. Dis.* 2012; **6**: 107–14.
13 Abbott DE, Bailey CM, Postovit LM, Seftor EA, Margaryan N, Seftor RE, Hendrix MJ. The epigenetic influence of tumor and embryonic microenvironments: how different are they? *Cancer Microenviron.* 2008; **1**: 13–21.
14 Epstein Shochet G, Drucker L, Pomeranz M, Fishman A, Pasmanik-Chor M, Tartakover-Matalon S, Lishner M. First trimester human placenta prevents breast cancer cell attachment to the matrix: the role of extracellular matrix. *Mol. Carcinog.* 2017; **56**: 62–74.
15 Epstein Shochet G, Brook E, Israeli-Shani L, Edelstein E, Shitrit D. Fibroblast paracrine TNF-alpha signaling elevates integrin A5 expression in idiopathic pulmonary fibrosis (IPF). *Respir. Res.* 2017; **18**: 122.
16 O'Reilly S, Ciechomska M, Cant R, van Laar JM. Interleukin-6 (IL-6) trans signaling drives a STAT3-dependent pathway that leads to hyperactive transforming growth factor-beta (TGF-beta) signaling promoting SMAD3 activation and fibrosis via Gremlin protein. *J. Biol. Chem.* 2014; **289**: 9952–60.
17 Gu L, Zhu YJ, Yang X, Guo ZJ, Xu WB, Tian XL. Effect of TGF-beta/Smad signaling pathway on lung myofibroblast differentiation. *Acta Pharmacol. Sin.* 2007; **28**: 382–91.
18 Mao Y, Schwarzbauer JE. Stimulatory effects of a three-dimensional microenvironment on cell-mediated fibronectin fibrillogenesis. *J. Cell Sci.* 2005; **118**(Pt 19): 4427–36.
19 Ekert JE, Johnson K, Strake B, Pardinas J, Jarantow S, Perkinson R, Colter DC. Three-dimensional lung tumor microenvironment modulates therapeutic compound responsiveness in vitro – implication for drug development. *PLoS One* 2014; **9**: e92248.
20 Larsson O, Diebold D, Fan D, Peterson M, Nho RS, Bitterman PB, Henke CA. Fibrotic myofibroblasts manifest genome-wide derangements of translational control. *PLoS One* 2008; **3**: e3220.
21 Parker MW, Rossi D, Peterson M, Smith K, Sikstrom K, White ES, Connett JE, Henke CA, Larsson O, Bitterman PB. Fibrotic extracellular matrix activates a profibrotic positive feedback loop. *J. Clin. Invest.* 2014; **124**: 1622–35.
22 Hinz B, Phan SH, Thannickal VJ, Prunotto M, Desmouliere A, Varga J, De Wever O, Mareel M, Gabbiani G. Recent developments in myofibroblast biology: paradigms for connective tissue remodeling. *Am. J. Pathol.* 2012; **180**: 1340–55.
23 Vaughan MB, Howard EW, Tomasek JJ. Transforming growth factor-beta1 promotes the morphological and functional differentiation of the myofibroblast. *Exp. Cell Res.* 2000; **257**: 180–9.
24 Hinz B, Celetta G, Tomasek JJ, Gabbiani G, Chaponnier C. Alpha-smooth muscle actin expression upregulates fibroblast contractile activity. *Mol. Biol. Cell* 2001; **12**: 2730–41.
25 Sarrazy V, Billet F, Micallef L, Coulomb B, Desmouliere A. Mechanisms of pathological scarring: role of myofibroblasts and current developments. *Wound Repair Regen.* 2011; **19**(Suppl. 1): s10–5.
26 Liu F, Mih JD, Shea BS, Kho AT, Sharif AS, Tager AM, Tschumperlin DJ. Feedback amplification of fibrosis through matrix stiffening and COX-2 suppression. *J. Cell Biol.* 2010; **190**: 693–706.
27 Nagahama KY, Togo S, Holz O, Magnussen H, Liu X, Seyama K, Takahashi K, Rennard SI. Oncostatin M modulates fibroblast function via signal transducers and activators of transcription proteins-3. *Am. J. Respir. Cell Mol. Biol.* 2013; **49**: 582–91.
28 Dees C, Tomcik M, Palumbo-Zerr K, Distler A, Beyer C, Lang V, Horn A, Zerr P, Zwerina J, Gelse K *et al.* JAK-2 as a novel mediator of the profibrotic effects of transforming growth factor beta in systemic sclerosis. *Arthritis Rheum.* 2012; **64**: 3006–15.
29 Pechkovsky DV, Prele CM, Wong J, Hogaboam CM, McAnulty RJ, Laurent GJ, Zhang SS, Selman M, Mutsaers SE, Knight DA. STAT3-mediated signaling dysregulates lung fibroblast-myofibroblast activation and differentiation in UIP/IPF. *Am. J. Pathol.* 2012; **180**: 1398–412.
30 Mross K, Stefanic M, Gmehling D, Frost A, Baas F, Unger C, Strecker R, Henning J, Gaschler-Markefski B, Stopfer P *et al.* study of the angiogenesis inhibitor BIBF 1120 in patients with advanced solid tumors. *Clin. Cancer Res.* 2010; **16**: 311–9.
31 Eisen T, Shparyk Y, Macleod N, Jones R, Wallenstein G, Temple G, Khder Y, Dallinger C, Studeny M, Loembe AB *et al.* Effect of small angiokinase inhibitor nintedanib (BIBF 1120) on QT interval in patients with previously untreated, advanced renal cell cancer in an open-label, phase II study. *Invest. New Drugs* 2013; **31**: 1283–93.
32 Rangarajan S, Kurundkar A, Kurundkar D, Bernard K, Sanders YY, Ding Q, Antony VB, Zhang J, Zmijewski J, Thannickal VJ. Novel mechanisms for the antifibrotic action of nintedanib. *Am. J. Respir. Cell Mol. Biol.* 2016; **54**: 51–9.
33 Huang RY, Kuay KT, Tan TZ, Asad M, Tang HM, Ng AH, Ye J, Chung VY, Thiery JP. Functional relevance of a six mesenchymal gene signature in epithelial-mesenchymal transition (EMT) reversal by the triple angiokinase inhibitor, nintedanib (BIBF1120). *Oncotarget* 2015; **6**: 22098–113.
34 Tai WT, Shiau CW, Li YS, Chang CW, Huang JW, Hsueh TT, Yu HC, Chen KF. Nintedanib (BIBF-1120) inhibits hepatocellular carcinoma growth independent of angiokinase activity. *J. Hepatol.* 2014; **61**: 89–97.
35 Lehtonen ST, Veijola A, Karvonen H, Lappi-Blanco E, Sormunen R, Korpela S, Zagai U, Skold MC, Kaarteenaho R. Pirfenidone and nintedanib modulate properties of fibroblasts and myofibroblasts in idiopathic pulmonary fibrosis. *Respir. Res.* 2016; **17**: 14.
36 Hisatomi K, Mukae H, Sakamoto N, Ishimatsu Y, Kakugawa T, Hara S, Fujita H, Nakamichi S, Oku H, Urata Y *et al.* Pirfenidone inhibits TGF-beta1-induced over-expression of collagen type I and heat shock protein 47 in A549 cells. *BMC Pulm. Med.* 2012; **12**: 24.
37 Conte E, Gili E, Fagone E, Fruciano M, Iemmolo M, Vancheri C. Effect of pirfenidone on proliferation, TGF-beta-induced myofibroblast differentiation and fibrogenic activity of primary human lung fibroblasts. *Eur. J. Pharm. Sci.* 2014; **58**: 13–9.
38 Nakazato H, Oku H, Yamane S, Tsuruta Y, Suzuki R. A novel anti-fibrotic agent pirfenidone suppresses tumor necrosis factor-alpha at the translational level. *Eur. J. Pharmacol.* 2002; **446**: 177–85.

